İSTANBUL UNIVERSITY CERRAHPAŞA

ORIGINAL ARTICLE
Electrica 2024; 24(1): 247-255

Load Cell-Based Two-Wheeled Mobile Robot Control with Proportion al–Integral–Derivative and Fuzzy Proportional–Integral–Derivative Methods

Muhammed Mustafa Kelek[1], Yüksel Oğuz[1], Uğur Fidan[2], Tolga Özer[1]

[1]Department of Electrical and Electronics Engineering, Afyon Kocatepe University Faculty of Technology, Afyonkarahisar, Türkiye
[2]Department of Biomedical Engineering, Afyon Kocatepe University Faculty of Engineering, Afyonkarahisar, Türkiye

Cite this article as: M. M. Kelek, Y. Oğuz, U. Fidan and T. Özer, "Load cell-based two-wheeled mobile robot control with proportional–integral–derivative and fuzzy proportional–integral–derivative methods," *Electrica*, 24(1), 247-255, 2024.

ABSTRACT

In this study, the two-wheeled mobile robot (TWMR) was controlled by taking the user's mass and center of gravity as a reference instead of the joystick control of the TWMR. A load-cell-based original TWMR system was proposed and realized. The behavior of the driving dynamics was discussed with a developed method different from other studies. The mathematical model of a load cell-based TWMR system was created and then simulated in the Matlab Simulink environment. This feature allowed the system to be more controlled and stable. The designed TWMR systems were controlled with proportional, integral, and derivative (PID) and fuzzy-PID controllers in the simulation. PID parameters in the system vary according to the mass of the user. The change of PID parameters was provided according to the mass information obtained from the load cell with the fuzzy-PID controller. Thus, the ability of the system to stay in balance was increased. Additionally, the speed of the TWMR and the pitching angle were controlled using PID and fuzzy-PID methods. The current values drawn from the battery were determined according to the applied controllers on 0° and 3° slope roads. The speed control of the motors was carried out with a mean error of 2%. The results of the fuzzy-PID control were observed to be better than those of the traditional PID controller.

***Index Terms*—**Control design, fuzzy & pid control, mobile robots, robot control, simulation

I. INTRODUCTION

Developed societies prefer to use electric vehicles in the transportation and service sectors because petroleum products increase air pollution and have low mechanical efficiency. The two-wheeled balance robot named Segway, which entered the literature for the first time in 2001, was used as a vehicle or mobile robot [1]. These vehicles are easy, practical, light, and easy to move even in small spaces, which provides a significant advantage in their usage. In addition, the absence of exhaust emissions increases interest in these vehicles daily. Due to these features, two-wheeled mobile robots (TWMR) have become preferred in various usage areas, such as airports, security forces, entertainment sectors, and factories. The control of TWMRs works according to the inverted pendulum principle. The balance of the system is realized with the help of control algorithms according to the data from the gyroscope sensor [2–4]. Different control techniques could be used for TWMR systems. Proportional, integral, and derivative controller (PID), linear quadratic regulator (LQR), Fuzzy logic controller (FLC), and artificial neural network (ANN) based controller designs were used in the control of TWMRs [2–15].

Sen investigated the effectiveness of FLC and LQR algorithms on the control of a two-wheeled balance robot. In his study, the bee algorithm was used to determine the FLC parameters, and the performances of the FLC and LQR algorithms were compared in a Matlab/Simulink environment. It is due to this comparison [16]. Pham et al. developed a ball-type TWMR. They provided the TWMR to move stably in the vertical position by using the hierarchical sliding mode control method in the simulation and application of the system [17]. Yoo et al. developed an FLC-based system for position and balance control of a TWMR-type mobile robot. They used a single-input FLC instead of the classical two-input FLC. It was observed that a single-input FLC offered similar control performance to conventional two-input FLC systems when the experimental results were compared [18]. Mohammed and Abdulla reached the performance ratios

Corresponding author:
Muhammed Mustafa Kelek

E-mail:
mmustafakelek@aku.edu.tr

Received: June 21, 2023

Revision Requested: September 4, 2023

Accepted: November 28, 2023

Publication Date: January 31, 2024

DOI: 10.5152/electrica.2024.23085

between genetic algorithm (GA) optimization and bacterial swarm (BS) optimization of LQR on the TWMR control. It was shown that BS more stably controls the system, responds faster, and balances more quickly [19]. Prabhakar et al. modeled and carried out the TWMR system. PID, GA-based PID, and Model Predictive Control (MPC) methods were applied to the Arduino-based control system. The MPC method was determined to be more successful than other control methods [20]. Ahmed compared the performance of TWMR using a classic-type PID and an ANN-based controller. His study aimed to control the pitching angle with the position of the joystick of the TWMR and make the system move more stable [13]. TWMRs provide many advantages in terms of usage area and functions. However, they have some disadvantages. One of the most important disadvantages of TWMRs is the accidents that may occur during usage. These accidents can cause traumatic injuries to the user.

Pourmand et al. analyzed the accidents with TWMR between 1990 and 2017 through academic studies published in PubMed. Their study emphasized that the TWMR was innovative, but the casualties were dangerous and had high treatment costs [21]. Dhillon and colleagues studied electric scooter accidents in Southern California between January and November 2018, and 87 accidents occurred during this time. 17.2% of the patients had a surgical operation. In addition, one accident resulted in death [22]. Yun et al. designed and controlled the serial elastic actuator (SEA) mechanism to improve the stability of the TWMR while in motion. Using SEA, the inertial force acting on the driver could be balanced up to 110 kg·m/s^2 in case of sudden acceleration or deceleration. The centrifugal force was compensated by more than 33.5% at the rotation moment [23]. Bang et al. developed an algorithm to precisely perform the TWMR's turn operations using the SEA-based TWMR. The control structure was created by placing four SEAs under the footplate [24]. The mean angle error value in the TWMR system was approximately 7% using the developed algorithm. There are various studies with load cells [25,26]. However, these studies have differences with this study in terms of mechanics, usage area, and control method.

In this study, load cells control the TWMR movement and balance by taking the user's center of mass and gravity information. Firstly, the mathematical model of a load cell-based TWMR system was created and then simulated in the Matlab Simulink environment. The load cells were used for orientation control of the TWMR. The output of the dynamic model of the system was updated according to the mass of the user. Thus, the maximum pitching angle is updated according to the user. It was thought that the possibility of users falling off the TWMR would be reduced with the update of the pitching angle. For this purpose, a load cell-based TWMR mechanical system design aimed at reducing accident rates was created and simulated successfully. TWMR motors were controlled with PID and fuzzy-PID controllers in the simulation. The simulated system's simulation results and performance rates were compared according to different driving dynamics.

II. TWO-WHEELED MOBILE ROBOT SYSTEM DESIGN

Brushless direct current (BLDC) motors are usually preferred for their efficiency, high torque, and simple maintenance [27]. Due to its features, the BLDC motor was selected as the actuator of TWMR in this study. This section explains the mathematical modeling of TWMR and the control of TWMR motors with PID and fuzzy-PID controller.

A. Mathematical Model of the Two-Wheeled Mobile Robot

The system was controlled with load cells placed on the TWMR [28]. The motors' torque values should have been calculated according to the torque–force relationship. Rolling, slope, air, and acceleration resistance forces are influential in the movement of the TWMR. The mathematical formulas for rolling and slope resistance forces are given in equations (1) and (2), respectively. The rolling resistance coefficient was taken as 0.012. This study ignored the effect of air and acceleration resistance forces on the TWMR.

$$F_R = f_r * G \tag{1}$$

$$F_{ST} = G * \sin\alpha \tag{2}$$

F_R represents the rolling resistance, F_{ST} is the slope resistance, f_r is the rolling resistance coefficient, G is the mass of the user, and α is the degree between the systems and the slope road. The F_R value varies according to the mass of the user, while the F_{ST} value varies depending on both the mass and the angle of the slope.

The system starts to move when the sum of the forces created by the TWMR motors is greater than the frictional forces acting on the system. The TWMR's pitching angle (Ψ) and steering angle (ϕ) must be calculated after the system moves. The pitching angle (Ψ) represents the angle created by the user when the user moves with their position perpendicular to the ground. It is shown in Fig. 1.

The mass of the user can be determined using the load cells. The user's maximum pitch angle (Ψmax) is calculated according to the mass information. Thus, it is foreseen to prevent the user from falling over this angle. Ψ_{max} differs for each user since Ψ_{max} depends on the user mass. This difference is perceived by the load cells, and the TWMR can be controlled adaptively. The physical representation of

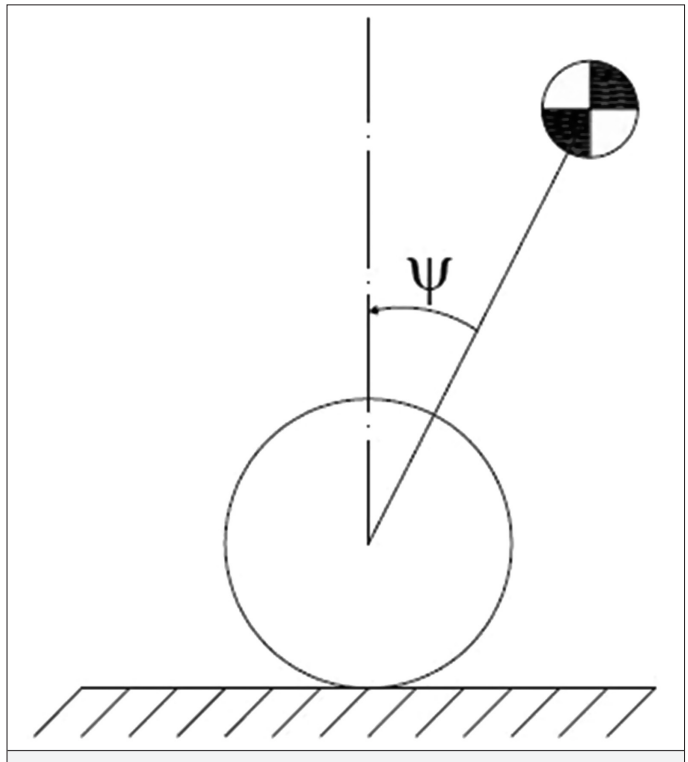

Fig. 1. The pitching angle of two-wheeled mobile robot system.

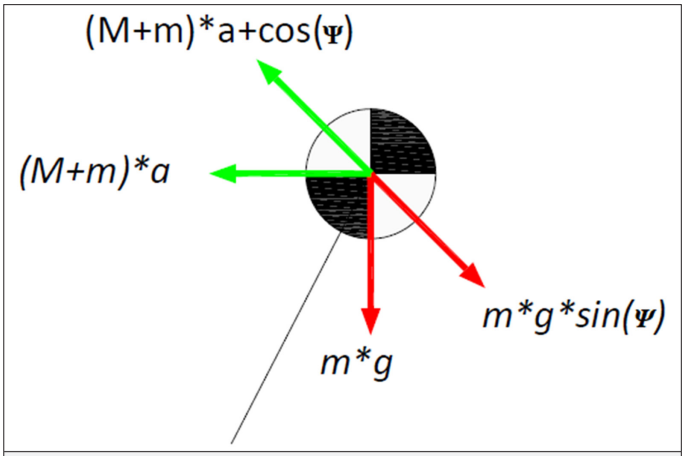

Fig. 2. The physical representation of the maximum pitching angle.

the Ψ_{max} is given in Fig. 2, and its mathematical equation is given in Equation (3).

$$\psi_{max} = \arctan\left(\frac{(M+m)*a}{M*g}\right) \quad (3)$$

The *m* represents the mass of the user, *M* is the mass of the TWMR, *a* is the acceleration, *g* is the gravitational acceleration, and Ψ is the pitch angle.

The motors' forces must be equally distributed when the TWMR steering angle (ϕ) is zero. However, in cases where the steering angle is different from zero, the motors' force–torque values should be produced, and the motors' speeds change. This study subtracted the steering angle from the pressure applied to the load cells. Thus, no additional external equipment is needed to calculate the steering angle. The pressure on each load cell determines the calculation of the steering angle. The right (w_{right}) and left (w_{left}) motor speeds of the TWMR are calculated after calculating the steering angle. The physical representation of the calculation for the right and left motor speeds is given in Fig. 3.

The mathematical formula of the right (w_{right}) and left (w_{left}) motor speeds according to the steering angle are given in equations (4–7):

$$x = L * \sin(\psi) \quad (4)$$

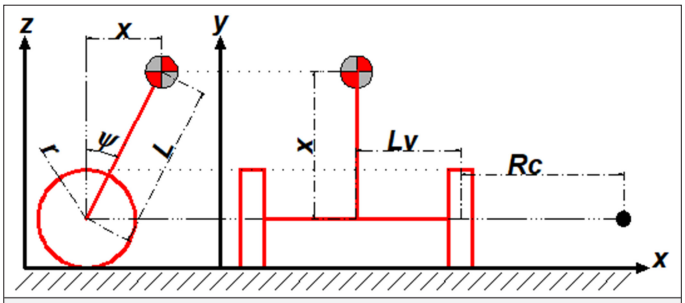

Fig. 3. Determination of right (w_{right}) and left (w_{left}) engine speeds according to the steering angle [28].

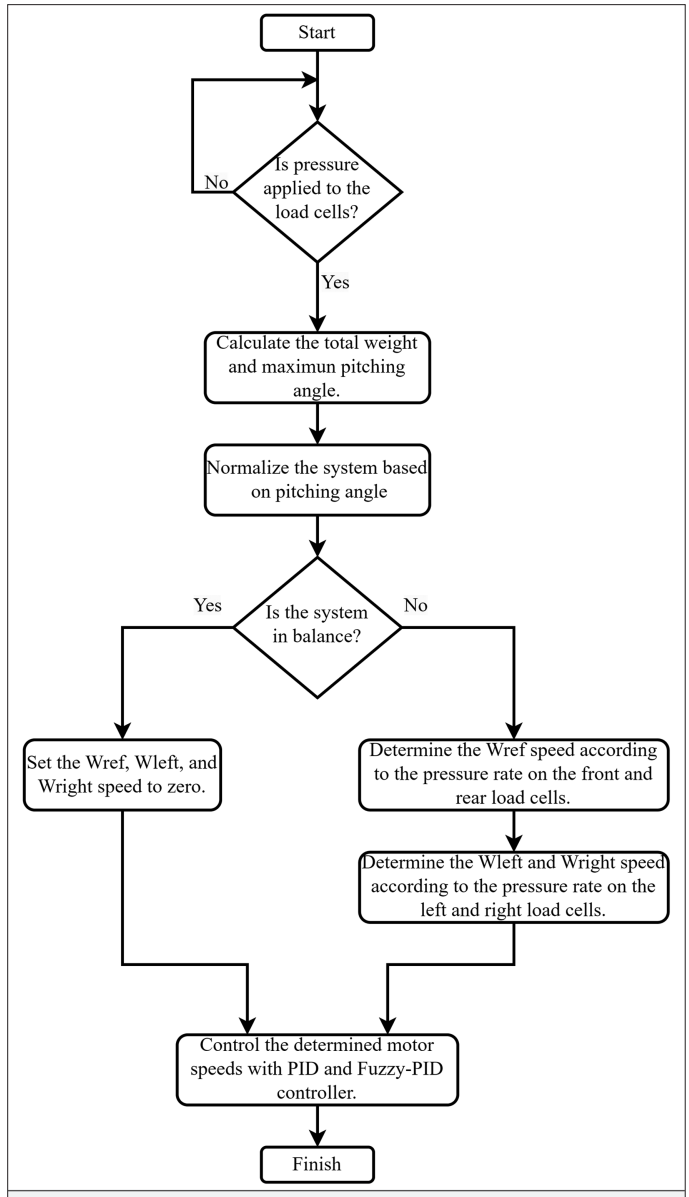

Fig. 4. Flowchart of the proposed two-wheeled mobile robot control algorithm.

$$\tan(d) = \frac{x}{(R_c + L_v)} \quad (5)$$

$$R_c = \left(\frac{L * \sin(\psi)}{\tan(d)}\right) - L_v \quad (6)$$

$$\frac{w_{ref}}{R_c + L_v} = \frac{w_{right}}{R_c} = \frac{w_{left}}{R_c + 2 * L_v} \quad (7)$$

Where *r* is the radius of the wheel (in Fig. 3), Ψ is the distance in the *z*-axis made by the user to the pitch attitude, *L* is the reach of the user's center of gravity to the TWMR, *x*: The distance on the *Z* axis when the TWMR tilts at a certain pitch angle, L_v is half of the TWMR floor length, and R_c is the size of the steering angle to the TWMR.

B. Two-Wheeled Mobile Robot Algorithm

The load cells are used in this proposed algorithm. The system is updated according to this weight by reaching the user's weight thanks to the load cells. Thus, a user-specific driving mode is created, allowing the user to drive better and more efficiently. First, the user is requested to put pressure on the load cells in the proposed algorithm. The motors are not allowed to be triggered without stressing all load cells. The purpose here is to prevent the user from falling by activating the motors while the user is getting on the TWMR. The mathematical calculations required for that mass are performed in the background, preventing the user from exceeding the maximum pitch attitude after the user's mass information is extracted. The system's control is realized by measuring the pressure distributions on the load cells. The ratio of the system's front and rear load cells determines the forward and backward movement of the TWMR, and the percentage of the load cells on the right and left facing each other determines the right and left orientation. The flow diagram of the proposed system is given in Fig. 4.

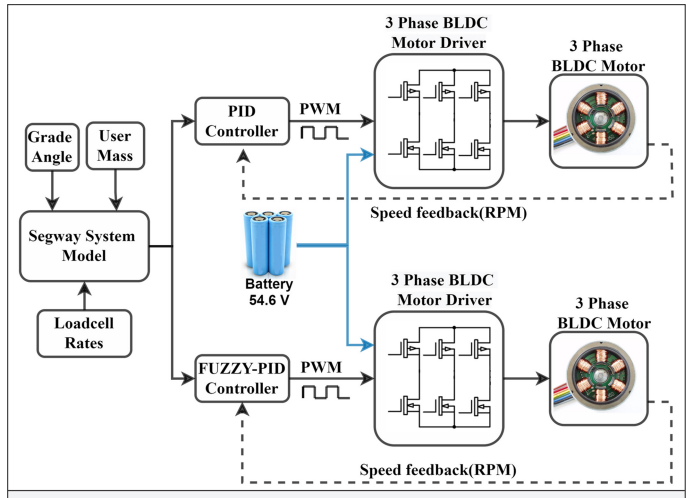

Fig. 5. Electrical block diagram of the designed system.

III. SIMULATION STUDY AND DISCUSSION

This section explained the simulation application of the load cell-based TWMR. A BLDC motor model with 320 rpm and 350 W motor power was used in the simulation of the TWMR, as used in the previous study [28]. The detailed BLDC motor specifications are given in [27]. The electrical block diagram of the designed system is shown in Fig. 5.

Phase triggers were made according to the data from the hall-effect sensor for the motor to work correctly. The Hall-effect sensor determines which of the windings in the BLDC is triggered. Current flows through two-phase windings in the motor using the data from three sensors. The other phase winding remains idle, and the motor continues to run. The microcontroller uses the information from the hall-effect sensors to determine which windings to trigger in the next step. Depending on the result of this process, control signals from the microcontroller trigger the switching components that allow current to flow through the relevant windings in the motor driver. Changes can be observed instantaneously in the simulation using various slide bars, as shown in Fig. 6.

The designed simulation application determined the PID coefficients with a fuzzy logic controller. Thus, PID parameters can adaptively update themselves according to the system. This feature gives the controlled system more successful results [29]. TWMR's motors were held according to the determined PID coefficients. The left motor of the TWMR was controlled with fuzzy-PID, and the right motor was controlled with PID in the simulation to see the difference between PID and fuzzy-PID controllers. The general block view of the TWMR simulation is given in Fig. 7.

The PID parameters of the right motor were determined by the trial-and-error method according to the pressures applied by the user to the load cells. The speed graphs of the motors were examined by randomly assigning the K_p, K_I, and K_D coefficients. The coefficient values that reach the desired speed fastest and make the most negligible overshoot and fluctuation are determined as PID parameters (Table I) when these graphs are examined. It is stated that other control methods are more complicated, complex, and challenging to implement than PID controller methods [30, 31].

The fuzzy-PID controller was used to control the left motor of the TWMR. There are two inputs for the fuzzy Logic controller: error (e) and instantaneous change of error (Δe). Seven membership

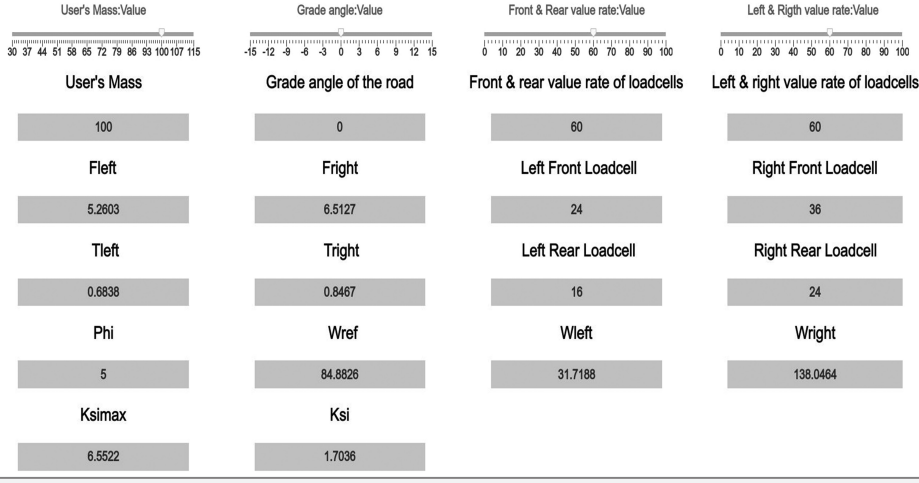

Fig. 6. Display the values that must be calculated instantly according to the user mass and load cell ratios.

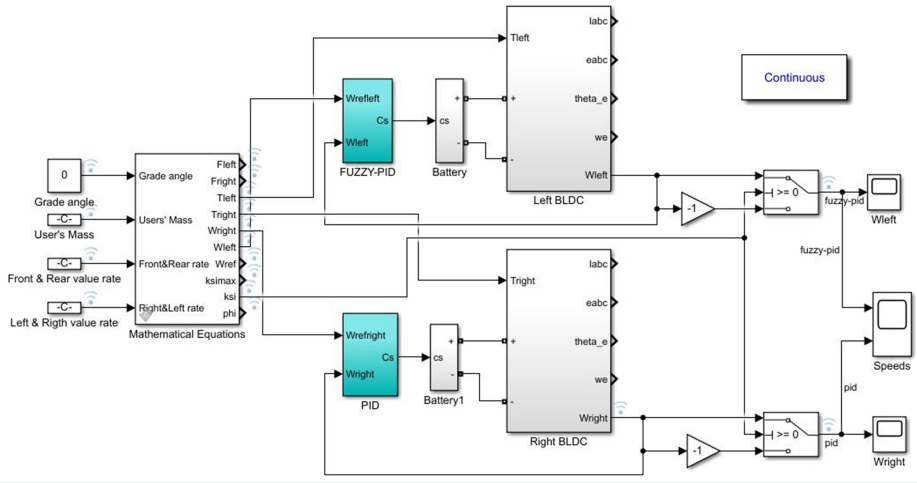

Fig. 7. The general view of the two-wheeled mobile robot simulation with fuzzy-PID and PID controller [28]. PID, Proportional, integral, and derivative.

TABLE I. PROPORTIONAL INTEGRAL DERIVATIVE PARAMETERS SET FOR USE IN THE CONTROL OF THE RIGHT MOTOR OF THE TWO-WHEELED MOBILE ROBOT

Proportional–Integral–Derivative Parameters	Value
K_p	10
K_I	$1e^{-5}$
K_D	$2.4e^{-2}$

functions were used for each input. These membership functions were named NB (Negative Big), NM (Negative Medium), NS (Negative Small), Z (Zero), PS (Positive Small), PM (Positive Medium), and PB (Positive Big). The triangle membership function type was used. A 7 × 7 rule table was created to determine the parameter values of the fuzzy-PID controller. The rule table for K_p, K_I, and K_D parameters is given in Table II.

Fuzzy-PID and PID controllers were compared as a result of the simulation. The time to reach the desired speed, the controllers' overshoot value and fluctuation values, and the motors' currents were obtained when the same reference speed values were given to users with different masses. In Fig. 8, the speeds are plotted so that users with masses of 30 kg (A) and 90 kg (B) reach the requested reference speed values. The TWMR was also tested on a straight road (0°) and a sloping road (3°).

When the test processes were examined, the speed of the motors reached approximately 250 rpm. It has been observed that the fuzzy-PID controller responds faster than the PID controller and gets the reference speed in a shorter time. It is determined that there is approximately a 3–5 rpm error rate when reaching the desired reference speeds. The error in the speed of the motor is related to the proportional coefficient of the fuzzy-PID controller. The coefficient of the proportional controller is high because it aims to reach the speed value at the desired reference speed in a short time. The mean speed error rate was calculated according to the error value of 5 rpm and was found to be 1.96%.

The change of graph in pitching angles obtained from the driving of 30 and 90 kg users according to different reference speeds is given in Fig. 9. Simulation tests were carried out at 4 different reference speeds: 250, 128, 169, and 45 rpm. Initially, the test was performed based on a reference speed of 250 rpm in the 0–2 second range. The pitching angle of the user with a mass of 30 kg is 6.3839, and the

TABLE II. PROPORTIONAL–INTEGRAL–DERIVATIVE PARAMETERS SET FOR USE IN THE CONTROL OF THE RIGHT MOTOR OF THE TWO-WHEELED MOBILE ROBOT

K_P-K_I-K_D	NB	NM	NS	Z	PS	PM	PB
NB	NB-NB-PS	NM-NB-NS	NS-NB-NB	NB-NB-NB	NS-NB-NB	NM-NB-NM	NB-NB-PS
NM	NM-PM-PS	NM-PM-NS	NS-PB-NB	NS-PB-NM	NS-PB-NM	NM-PM-NS	NM-PM-Z
NS	NS-PM-Z	NS-PB-NS	NS-PB-NB	Z-PB-NM	NS-PB-NS	NS-PB-Z	NS-PM-Z
Z	NM-PB-NS	NM-PB-NS	Z-PM-NS	Z-Z-NS	Z-PM-NS	PM-PB-Z	PM-PB-Z
PS	PM-PM-Z	PS-PB-Z	PS-PB-Z	Z-PB-Z	PS-PB-Z	PS-PB-PB	PM-PM-NS
PM	PM-PM-PS	PM-PM-PS	PS-PB-PS	PS-PB-PS	PS-PB-PB	PM-PM-PB	PM-PM-PM
PB	PB-NB-PM	PB-NB-PM	PB-NB-PS	PB-NB-PS	PB-NB-PB	PB-NB-Z	PB-NB-NS

NB, Negative Big; NM, Negative Medium; NS, Negative Small; PB, Positive Big; PM, Positive Medium; PS, Positive Small; Z, Zero.

pitching angle of the user with a mass of 90 kg is 5.2920. It was determined that the pitching angle of the user with a mass of 30 kg was

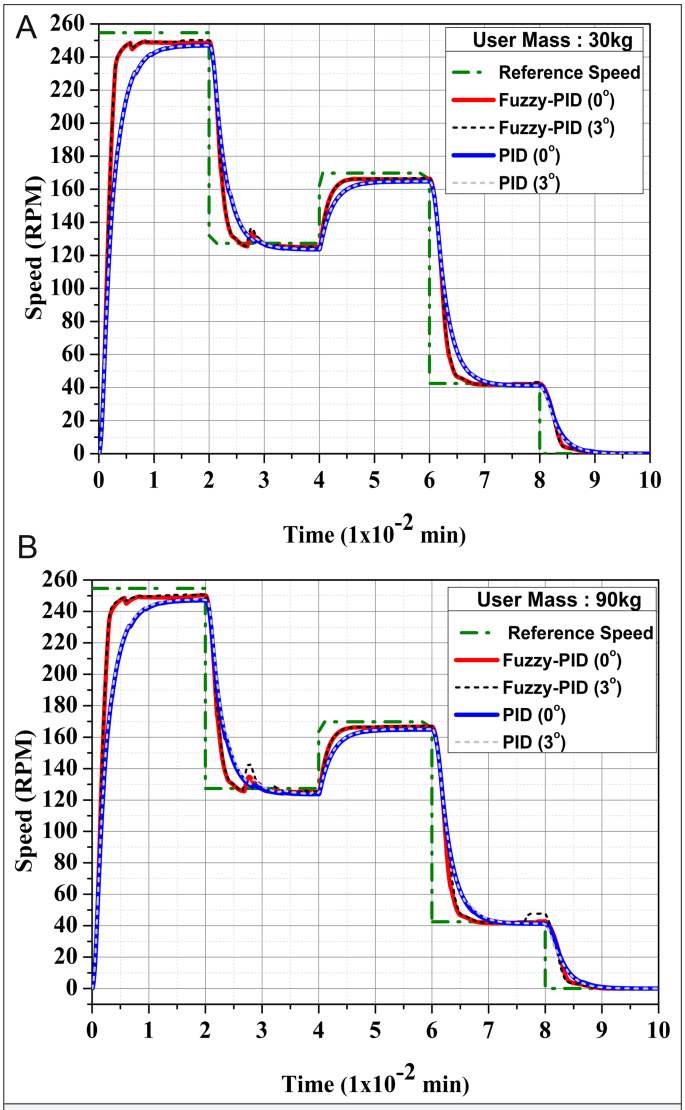

Fig. 8. Speed graph of two-wheeled mobile robot on 0° and 3° slopes for 30 kg (a) and 90 kg (b) masses users.

3.2416, while the pitching angle of the user with a 90 kg mass was 2.7589 based on the 128 rpm reference speed in the range of 2–4 seconds. In the 4–6 second interval, the pitching angle of the 30 kg user was 4.2561, and the 90 kg user's pitching angle was 3.5153 at 169 rpm. Finally, it has been determined that the pitching angle of the user with a mass of 30 kg is 1.1026 at a speed of 45 rpm, while the pitching angle of the user with a mass of 90 kg is 0.9843. It is seen that the pitching angle value changes depending on the reference speed in the use of the TWMR. The difference in pitching angle values between users with 30 and 90 kg of mass increases as the reference speed increases. It is seen that the pitching angle of the user with a mass of 30 kg is higher than that of the user with a mass of 90 kg.

The force applied to the front and rear load cells changed the pitching angle. The relation between user mass and pitching angle is

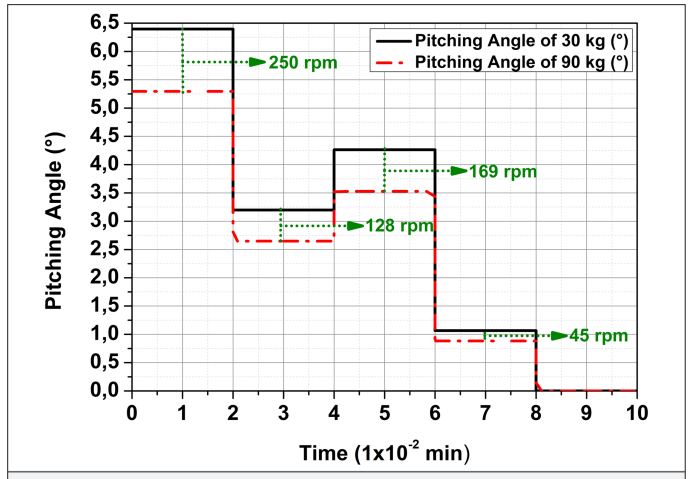

Fig. 9. Variation of pitching angle obtained for different reference speeds with 30 and 90 kg users.

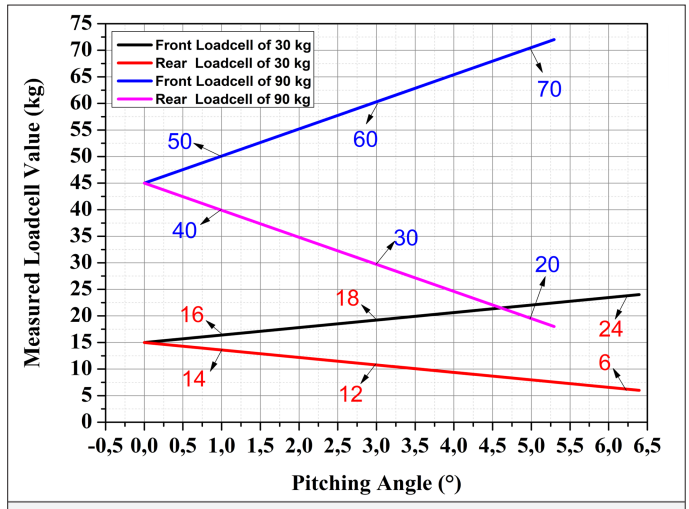

Fig. 10. Change of pitching angle according to variable load distribution in front and rear load cells.

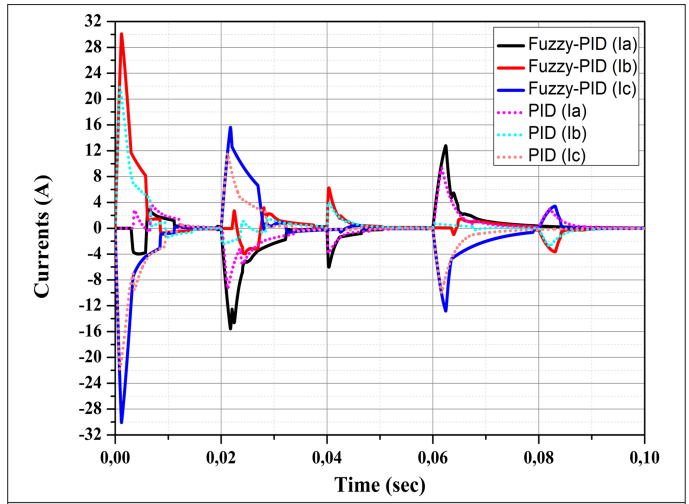

Fig. 11. Currents of fuzzy proportional–integral–derivative and proportional–integral–derivative controller for the 30 kg mass user.

TABLE III. MOTORS DRAW CURRENT VALUES ACCORDING TO CONTROL TYPE AT DIFFERENT MASSES AND SLOPES

User Masses	Type of the Controller	Current Values Drawn by Motors at 0° Slope Road	Current Values Drawn by Motors at 3° Slope Road
30 kg	PID controller	3.98894	4.37206
	Fuzzy-PID controller	5.45526	6.31083
45 kg	PID Controller	4.01036	4.71966
	Fuzzy-PID controller	5.58470	6.82952
60 kg	PID controller	4.04046	5.14126
	Fuzzy-PID controller	5.64873	7.47302
75 kg	PID controller	4.07946	5.59763
	Fuzzy-PID controller	5.72297	7.96175
90 kg	PID controller	4.12175	6.07706
	Fuzzy-PID controller	5.83469	8.30407

PID, proportional–integral–derivative.

shown in Fig. 10 with 2 different user masses. The user can achieve the same speed with less pitching angle value to perform the forward movement when the mass of the user increases. The pitching angle required for high-mass users to reach the specified speed value is lower than for low-mass users. So, it is understood that the risk of falling off the TWMR for high-mass users is reduced.

The current information was obtained from the user's driving on 0° and 3° sloping roads. Fuzzy-PID controls TWMR, and the PID controller during the TWMR driver mass is 30 kg. The current graph of the motors is given in Fig. 11 with a 0° slope road. Average drawn current values according to different user masses and slopes are presented in Table III.

The proportions between the flow and the mass information are given in Table III. As a result of the examination, the correlation value between the user mass on the 0° sloping road and the current values drawn by the PID-controlled TWMR was $R2 = 0.9836$. The correlation coefficient between the user mass and the current drawn by the TWMR motors controlled by fuzzy-PID on the 0° sloping road was $R2 = 0.9861$. As can be seen, the similarity ratio between the user mass and the current drawn from the motor controlled by the fuzzy-PID controller increased even more on the 0° sloping road. The current values of the motor controlled by fuzzy-PID are higher than those of the PID control method. It is understood from Fig. 11 and Table III that the fuzzy-PID control method responds faster to sudden changes in the system and accordingly draws a higher current.

This study created a mechanical system using load cells, and the system's control was carried out in a simulation environment. The mean speed error rate was calculated at 1.96%. Hence, the system's ability to balance was increased, and the risk of a TWMR accident was reduced. In addition, the speed of the TWMR, the current values drawn from the motors, and the pitching angle were controlled using PID and fuzzy-PID control methods. The current values drawn from the battery were determined according to the controllers applied on 0° and 3° sloping roads. Fuzzy-PID controls the motors with a mean error of 2%. It was observed that the fuzzy-PID controller type was better than the traditional PID controller, according to the obtained simulation results.

IV. CONCLUSION

In this study, the load cell-based TWMR was controlled in a simulation environment with fuzzy-PID and PID control algorithms. The fuzzy-PID controller, which could change the parameters according to the PID control method, was observed to give better results. The settling time of the TWMR motor controlled by the fuzzy-PID control algorithm was faster than PID control. There were 3–5 rpm fluctuations in speed due to this quick response time. Motor currents were measured on TWMR's straight (0°) and sloping (3°) roads with different user masses. It was seen that a more stable system could be obtained with the application of the proposed control method. Thus, it was foreseen that the accidents that may occur with the TWMR could be reduced to a minimum.

Peer-review: Externally peer-reviewed.

Author Contributions: Concept – M.M.K., T.O.; Design – M.M.K., U.F.; Supervision – Y.O., U.F.; Materials – T.O., M.M.K.; Analysis and/or Interpretation – Y.O., U.F., M.M.K.; Literature Search – T.O., M.M.K.; Writing Manuscript – M.M.K., T.O.; Critical Review – Y.O., U.F.

Declaration of Interests: The authors have no conflict of interest to declare.

Funding: The authors declared that this study has received no financial support.

REFERENCES

1. D. L. Kamen *et al.*, U.S. Patent No: 6, 302,230. U.S. Patent and Trademark Office. Washington, DC, 2001.
2. C. H. Chiu, and Y. F. Peng, "Design and implement of the self-dynamic controller for two-wheel transporter," 2006 IEEE International Conference on Fuzzy Systems, Vancouver BC, CA, 480–483, 2006. [CrossRef]
3. S. Jeong, and T. Takahashi, "Wheeled inverted pendulum type assistant robot: Inverted mobile, standing and sitting motions." 2007 IEEE/RSJ International Conference on Intelligent Robots and Systems, San Diego CA, USA, 2007, 2007. [CrossRef]

4. R. Grepl, "Balancing wheeled robot: Effective modelling sensory processing and simplified control," *Eng. Mech.*, vol. 16, no. 2, pp. 141–154, 2009.
5. C. E. Forrest, *A Neural Network Control System for the Segway Robotic Mobility Platform*, MS Thesis. Raleigh, USA: Comput, NC State University, 2006.
6. L. J. Butler, and G. Bright, "Feedback control of a self-balancing materials handling robot," 10th International Conference on Control, Automation, Robotics and Vision, Hanoi, Vietnam, 2008. [CrossRef]
7. D. Küçük, *Design of Two Wheeled Twin Rotored Hybrid Robotic Platform*, MS Thesis. İstanbul, Türkiye: Atilim University, 2010.
8. M. U. Draz, M. S. Ali, M. Majeed, U. Ejaz, and U. Izhar, "Segway electric vehicle." 2012 International Conference of Robotics and Artificial Intelligence, Rawalpindi, Pakistan, 2012, 2012. [CrossRef]
9. M. Han, K. Kim, D. Y. Kim, and J. Lee, "Implementation of unicycle SEGWAY using unscented Kalman filter in LQR control," In 2013 10th International Conference on Ubiquitous Robots and Ambient Intelligence (URAI), Jeju, Korea, 2013, 2013. [CrossRef]
10. D. B. Pham, H. Kim, J. Kim, and S. G. Lee, "Balancing and transferring control of a ball SEGWAY using a double-loop approach [applications of control]," *IEEE Control Syst.*, vol. 38, no. 2, pp. 15–37, 2018. [CrossRef]
11. M. Steiner, *ROS Navigation Stack on A Loomo SEGWAY Robot*, BS Thesis. Munich, Vienna: Vienna University, 2018.
12. J. Morantes, D. Espitia, O. Morales, R. Jiménez, and O. Aviles, "Control system for a segway", *IJAER*, Vol. 13, no. 18, pp. 13767–13771, 2018.
13. A. A. Ahmed, and A. F. S. Alshandoli, "On replacing a PID controller with Neural Network controller for segway." 2020 International Conference on Electrical Engineering (ICEE), Istanbul, Türkiye, 2020. [CrossRef]
14. S. R. Vaishnav, and Z. J. Khan, "Design and performance of PID and fuzzy logic controller with smaller rule set for higher order system," in Proceedings of the World Congress on Engineering and Computer Science, San Francisco, USA, 2007.
15. M. M. Kelek, Y. Oguz, U. Fidan, and T. Özer, "'Real-time control of load cell based segway using PID controller', PAJES," *Pamukkale J. Eng. Sci.*, vol. 27, no. 5, pp. 597–603, 2021. [CrossRef]
16. M. A. Şen, *Design and Optimization of a Fuzzy Logic-Based Controller for a Two-Wheeled Robot by Using the Bees Algorithm*, MS Thesis. Konya, Türkiye: Selcuk University, 2014.
17. D. B. Pham, and S. G. Lee, "Hierarchical sliding mode control for a two-dimensional ball SEGWAY that is a class of a second-order underactuated system," *Vib. Control*, vol. 25, no. 1, pp. 72–83, 2019. [CrossRef]
18. H. H. Yoo, and B. J. Choi, "Design of simple-structured fuzzy logic systems for segway-type mobile robot," *Int. J. Fuzzy Log. Intell. Syst.*, vol. 15, no. 4, pp. 232–239, 2015. [CrossRef]
19. I. K. Mohammed, and A. I. Abdulla, "Balancing a SEGWAY robot using LQR controller based on genetic and bacteria foraging optimization algorithms," *Telkomnika*, vol. 18, no. 5, pp. 2642–2653, 2020. [CrossRef]
20. G. Prabhakar, S. Selvaperumal, P. N. Pugazhenthi, K. Umamaheswari, and P. Elamurugan, "Online optimization-based model predictive control on two-wheel segway system," *Mater. Today*, vol. 33, no. 1, pp. 3846–3853, 2020. [CrossRef]
21. A. Pourmand, J. Liao, J. M. Pines, and M. Mazer-Amirshahi, "SEGWAY® personal transporter-related injuries: A systematic literature review and implications for acute and emergency care," *J. Emerg. Med.*, vol. 54, no. 5, pp. 630–635, 2018. [CrossRef]
22. N. K. Dhillon et. al., "Electric scooter injury in Southern California trauma centers," *J. Am. Coll. Surg.*, vol. 231, no. 1, pp. 133–138, 2020. [CrossRef]
23. H. Yun, J. Bang, J. Kim, and J. Lee, "High speed segway control with series elastic actuator for driving stability improvement," *J. Mech. Sci. Technol.*, vol. 33, no. 11, pp. 5449–5459, 2019. [CrossRef]
24. J. U. Bang, J. H. Kim, and J. Lee, "Precise curve motion control of a SEGWAY by compensating the centrifugal force with SEAs," *Int. J. Control Autom. Syst.*, vol. 19, no. 6, pp. 2018–2025, 2021. [CrossRef]
25. M. Suzuki, S. Yokota, A. Matsumoto, D. Chugo, and H. Hashimoto, "Simulation of Omni-Directional Low-Floor Mobility Controlled by Inverted Pendulum and Human Postural Control Model in forward-backward direction," IECON 2020 The 46th Annual Conference of the IEEE Industrial Electronics Society, Singapore, 2020, pp. 2668–2674. [CrossRef]
26. S. Naruoka, N. Takesue, and D. Kobayashi, "Improvement of straight-line movement of personal vehicle on water using yaw-rate feedback," 2018 12th France-Japan and 10th Europe-Asia Congress on Mechatronics, Tsu, Japan, pp. 411–414, 2018. [CrossRef]
27. M. M. Kelek, İ. Çelik, U. Fidan, and Y. Oğuz, "The simulation of mathematical model of outer rotor BLDC motor", 4th International Symposium on Innovative Approaches in Engineering and Natural Sciences, Samsun, Türkiye, 2019. [CrossRef]
28. M. M. Kelek, U. Fidan, Y. Oğuz, I. Celik, and T. Özer, "Load cell-based PID method-controlled segway system modelling and simulation," *IJESMS*, vol. 12, no. 4, pp. 230–238, 2021. [CrossRef]
29. F. Katırcıoğlu, M. M. Kelek, M. Şen, I. Koyuncu, and Y. Oğuz, "FPGA-Based Design of Gaussian Membership Function for Real-Time Fuzzy Logic Applications," V. International Multidisciplinary Congress of Eurasia, Barcelona, Spain, 2018.
30. J. Zhang, N. Wang, and S. Wang, "A developed method of tuning PID controllers with fuzzy rules for integrating processes," in Proceedings of the American Control Conference, Boston, 2004. [CrossRef]
31. K. H. Ang, G. Chong, and Y. Li, "PID control system analysis, design and technology," *IEEE Trans. Control Syst. Technol.*, vol. 13, no. 4, pp. 559–576, 2005. [CrossRef]

M. Mustafa KELEK received an M. Sc in electrical and electronic engineering from Afyon Kocatepe University in 2020. He is a research assistant in the Electric and Electronic Engineering Department at Afyon Kocatepe University, Afyonkarahisar, Turkey. His research interests include robotics, embedded systems, and microcontroller-based control applications.

Yuksel Oguz received his M. Sc and Ph.D. in Electrical Education from the Marmara University, Institute for Graduate Studies in Pure and Applied Sciences, between 2000 and 2007. He is working as a Professor in the Electronic and Electronic Engineering Department at Afyon Kocatepe University. His research interests include control systems, automatic applications, electrical machines, and intelligent control systems.

Ugur Fidan has received his Ph.D. degree in the electronic computer education department from Gazi University. He is working as an Assoc. Prof. in the Biomedical Engineering department at Afyon Kocatepe University. His research interests include signal processing, embedded systems, and analog system design.

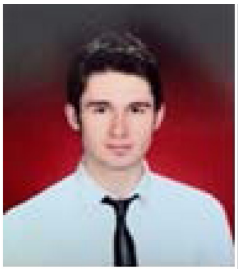

Tolga Ozer received a Ph.D. degree in electrical and electronic engineering from Ankara Yıdırım Beyazıt University. He is working as an Assist. Prof. in the Electric and Electronic Engineering Department, Afyon Kocatepe University, Afyonkarahisar, Turkey. His research interests include battery management systems, motor drivers, and micro-controller-based control applications.